Gating of the active site of triose phosphate isomerase: Brownian dynamics simulations of flexible peptide loops in the enzyme

Rebecca C. Wade, Malcolm E. Davis, Brock A. Luty, Jeffrey D. Madura, and J. Andrew McCammon
Department of Chemistry, University of Houston, Houston, Texas 77204-5641 USA

ABSTRACT The enzyme triose phosphate isomerase has flexible peptide loops at its active sites. The loops close over these sites upon substrate binding, suggesting that the dynamics of the loops could be of mechanistic and kinetic importance. To investigate these issues, the loop motions in the dimeric enzyme were simulated by Brownian dynamics. The two loops, one on each monomer, were represented by linear chains of appropriately parameterized spheres, each sphere corresponding to an amino acid residue. The loops moved in the electrostatic field of the rest of the enzyme, which was held rigid in its crystallographically observed conformation. In the absence of substrate, the loops exhibited gating of the active site with a period of about 1 ns and occupied "closed" conformations for about half of the time. As the period of gating is much shorter than the enzyme-substrate relaxation time, the motion of the loops does not reduce the rate constant for the approach of substrate from its simple diffusion-controlled value. This suggests that the flexible loops may have evolved to create the appropriate environment for catalysis while, at the same time, minimizing the kinetic penalty for gating the active site.

INTRODUCTION

Triose phosphate isomerase (TIM) (D-glyceraldehyde 3-phosphate ketol isomerase; EC 5.3.1.1), a glycolytic enzyme that catalyzes the interconversion of D-glyceraldehyde-3-phosphate (GAP) and dihydroxyacetone phosphate, has been described (1) as being an almost perfect catalyst because of its remarkable efficiency. The reaction appears to be diffusion controlled (2) and proceeds with a measured rate constant of $4.8 \times 10^8\ M^{-1}\ s^{-1}$ (1). TIM consequently has been the focus of a large number of kinetic and structural studies (3).

In a previous study (4), the diffusional encounter between TIM and GAP, which is the rate-limiting step of the reaction (1), was simulated using Brownian dynamics (BD). A rate constant of $1.5 \times 10^{10}\ M^{-1}\ s^{-1}$ was calculated, and electrostatic steering of the substrate by the enzyme was found to contribute to the high rate constant. This calculated rate constant is, however, 1–2 orders of magnitude greater than the experimental rate constant. This overestimation may be due to the simplicity of the model of the substrate-enzyme system used for the calculations that neglected certain important contributions.

One of these may be the effects of the mobile peptide loops that close over the active sites upon substrate binding (5); as in the previous study, the whole protein was treated as a rigid body. These loops are important in determining specificity for particular substrates, in stabilizing the reaction intermediates, and in excluding solvent from the active site (6). They must be in "open" conformations to allow substrate access to the active sites. These loops may influence the enzymatic rate constant in the following ways.

(*a*) Each loop could act as a gate over an active site and thus prevent substrate access when it is in a "closed" conformation. The motion of the loops could thus lead to a reduction in the rate constant.

(*b*) Each loop could perhaps serve as a "scoop" that guides the substrate into the active site. The loops could thus facilitate substrate access to the active sites and lead to an increase in the rate constant.

In this work, the motion of the peptide loops has been simulated in the absence of substrate to assess whether the loops can act as "gates" to the catalytic sites. In further work, in which the diffusive motion of both the substrate and the loops will be simulated, we plan to investigate whether the loops can assist the access of the substrate to the active sites.

We have used the BD simulation method because of the diffusion-controlled nature of the reaction and because of the long time scales of the motion of the peptide loops. Simulations of 70–100-ns duration were necessary, and such long times are beyond the scope of current molecular dynamics simulations, which are typically of the order of 100 ps. To achieve these time scales, a relatively simple model of the peptide loops was necessary. They were represented by linear chains of mobile spheres, each sphere representing one amino acid residue. These chains were attached at each end to the rest of the protein, which was held stationary in its crystallographically observed conformation. The motion of each of the spheres was governed by the electrostatic field of the stationary part of the protein, the forces due to the other mobile spheres, and the random forces due to solvent fluctuations.

In the next section, we give details of the model of the system and the simulation method. After this, we de-

Address correspondence to Rebecca C. Wade.
R. C. Wade's present address is European Molecular Biology Laboratory, Meyerhofstr. 1, 6900 Heidelberg, Germany.
M. E. Davis's present address is Bristol-Myers Squibb Pharmaceutical Research Institute, P.O. Box 4000, Princeton, NJ 08543.
J. D. Madura's present address is Department of Chemistry, University of South Alabama, Mobile, AL 36688.

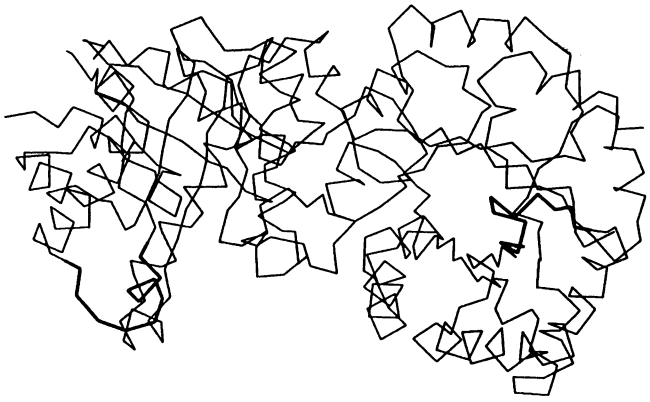

FIGURE 1 α-Carbon trace of the crystal structure of the chicken TIM dimer. The two simulated flexible peptide loops are shown by bold lines in "open" conformations.

scribe and discuss the resultant motion and the calculation of rate constants.

METHODS

Model

The structures of chicken (7), yeast (8, 9), and trypanosomal (10) TIMs have been solved by x-ray crystallography in their native forms as well as in the presence of a number of substrates and inhibitors. The calculations described in this article were done for chicken TIM, which was the only TIM crystal structure (7, 11, 12) available from the Brookhaven Protein Databank (13) (file 1TIM) at the time that this work was started.

TIM is a dimer, consisting of two identical polypeptide chains (subunits I and II) of 247 amino acid residues. Each subunit consists of eight loop-β-loop-α units and contains one active site (Fig. 1). Over each active site, there is a particularly long loop containing residues 168–176 (in the chicken TIM numbering scheme [7] in which residues are numbered 1–2 and 4–248) whose sequence is highly conserved. This has been shown experimentally to be flexible in the absence of substrate but to close over the active site into an ordered conformation on binding of substrate (12). Experimental (8) and theoretical evidence (14) suggests that the loop may act as a fairly rigid hinged "lid." In the crystal structure of chicken TIM (7, 11, 12), residues 168–176 are disordered in subunit I but are observed in a defined open conformation in subunit II.

In the work described here, all atoms of the chicken TIM dimer except those in the two simulated loops were held fixed in their crystallographically observed positions. Hydrogen atoms were added in appropriate positions using the QUANTA molecular modeling package (15). Assigning all titrating residues their usual protonation state at neutral pH, the approximate pH of solutions for crystallographic and kinetic studies of TIM, the complete enzyme was neutral and the fixed atoms had an overall charge of -2 e. Partial point charges and van der Waals radii were assigned to all atoms from the OPLS (16) parameter set. The electrostatic field of the fixed atoms was calculated by solving the linearized Poisson–Boltzmann (LPB) equation using a finite difference method (17). For this, TIM was placed in the center of a $110 \times 110 \times 110$ grid with a grid spacing of 1 Å. The excluded volume of the enzyme was calculated by identifying as excluded all grid points within a distance equal to the sum of the van der Waals radius of the atom nearest to the grid point plus 2 Å (the radius of a methyl group). The protein interior was assigned a relative dielectric constant of 2, and the surrounding exterior region was assigned a relative dielectric constant of 78. The relative dielectric constant was "smoothed" at the molecular surface so that it changed gradually between its two continuum values (18). The LPB equation was solved using boundary conditions at the edges of the grid for which the protein was assumed to be equivalent to a Debye–Huckel sphere with a radius of 40 Å. The electrostatic potential was calculated in the presence of solvents of zero and 0.1 M ionic strength without a Stern layer.

The peptide loops were modeled as linear chains of spheres connected by pseudobonds, with each sphere parameterized to represent one amino acid residue (Fig. 2). Each chain consisted of 17 residues (163–179) of which the central 11 residues (166–176) were allowed to move. The three residues at each end were held fixed but contributed to the forces on the mobile residues. The peptide loops were represented using a model developed by Levitt and Warshel (19, 20) and subsequently modified by McCammon et al. (21). All of the spheres had identical hydrodynamic radii of 3.15 Å, the radius assigned to threonine in this model (20). This radius was chosen because threonine was the residue that occurred with the greatest frequency in the loop (3 times in residues 163–179; Table 1) and was of intermediate size. Hydrodynamic interactions between the loop residues were neglected. A central point charge was assigned to each residue corresponding to its overall charge. In chicken TIM, only one of the mobile residues in each loop (Lys 174) had a formal charge.

Force field

The force on each residue i was given by:

$$\mathbf{F}_i = -\frac{\partial E(\boldsymbol{r}_i)}{\partial \boldsymbol{r}_i}, \qquad (1)$$

where the energy E of the moving residues consisted of the following components:

$$E = E^{\text{elec}} + E^{\text{bond}} + E^{\text{angle}} + E^{\text{nnnb}} + E^{\text{si}} + E^{\text{exv}}. \qquad (2)$$

These were given as follows:

$$E^{\text{elec}} = \sum_i E_i^{\text{LPB}} + \sum_i E_i^{\text{Coulomb}}. \qquad (3)$$

E_i^{LPB} is the energy of residue i with charge q_i in the electrostatic potential V of all the fixed atoms calculated using the LPB equation,

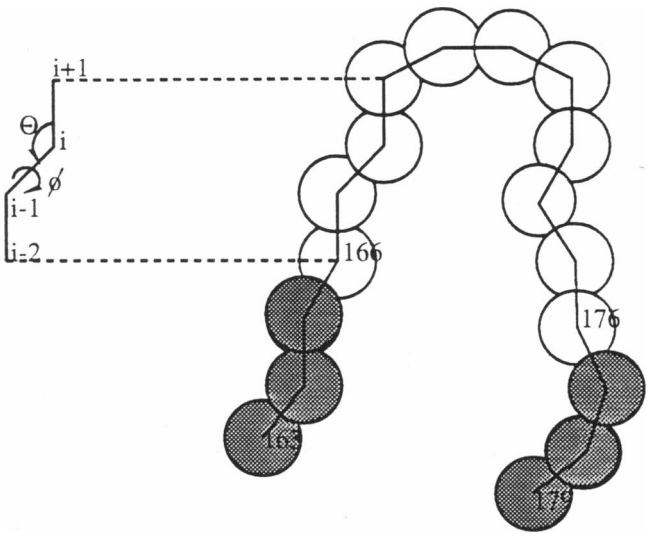

FIGURE 2 Representation of one peptide loop (residues 163–179) in the Brownian dynamics simulations. Each loop consists of 17 spheres, each sphere representing an amino acid residue. The three shaded spheres at each end of the loop are fixed and the central 11 are free to move. Angles Θ and ϕ are defined as shown in the figure.

TABLE 1 **Amino acid sequences of the simulated flexible peptide loop for the TIMs whose crystal structures have been solved**

Residue no.*			165					170					175				
Chicken	A	Y	E	P	V	W	A	I	G	T	G	K	T	A	T	P	Q
S. cerevisiae	A	Y	E	P	V	W	A	I	G	T	G	L	A	A	T	P	E
T. brucei	A	Y	E	P	V	W	A	I	G	T	G	K	V	A	T	P	Q
Consensus‡	A	Y	E	P	V	W	A	I	G	T	G	—	—	—	—	—	—

* The residues are numbered according to the convention in which the residues of chicken TIM are numbered 1–2 and 4–248.
‡ The consensus sequence is given for the 13 known TIM sequences.

$$E_i^{\mathrm{LPB}} = q_i V, \tag{4}$$

and E_i^{Coulomb} is the Coulombic point charge interaction between residue i and all the other residues j that are free to move.

$$E_i^{\mathrm{Coulomb}} = \sum_j \frac{q_i q_j}{4\pi\epsilon_0 \epsilon r_{ij}} \tag{5}$$

where r_{ij} is the distance between residues i and j, ϵ is the relative dielectric constant of the solvent, and ϵ_0 is the permittivity of free space. (Although some of the residues were separated by protein, it was assumed that most interactions were mediated by solvent.)

During equilibration, the energy of the pseudobonds was given by:

$$E^{\mathrm{bond}} = \sum_i \frac{k_b}{2}(b_i - b_0)^2 \tag{6}$$

where b = 5.14 Å and k_b = 80 kcal/mol/Å^2 (21). In the subsequent data collection simulations, E^{bond} was not evaluated; instead, the length of the pseudobonds between the spheres was maintained at 5.14 Å with a tolerance of 0.02 Å by means of corrections at each timestep using a modified SHAKE algorithm (22, 23, 31).

The energy arising from deviations of the angles Θ and ϕ (Fig. 2) from their optimal values was calculated for all angles j in each loop.

$$E^{\mathrm{angle}} = \sum_j \frac{k_\Theta}{2}(\Theta_j - \Theta_0)^2, \tag{7}$$

where Θ_0 = 1.52 rad (87.2°) and the force constant k_Θ = 80 kcal/mol/rad^2 (21).

E^{nnnb}, the nearest neighbor nonbonded term, was calculated for the dihedral angles ϕ defined for residues $i-2$, $i-1$, i, and $i+1$ with ϕ = 0° corresponding to the eclipsed conformation.

$$E^{\mathrm{nnnb}} = \sum_i 2 \sum_{k=1}^{6} A_k^i \cos[(k-1)\phi_i + B_k^i \sin[(k-1)\phi_i]. \tag{8}$$

The coefficients A_k^i and B_k^i are dependent on the identity of the third (ith) residue defining the dihedral angle. Coefficients corresponding to alanine were used for all residues except Gly and Pro, which had different coefficients. This term and these coefficients are given by Levitt (20).

E^{si} is a side chain solvent interaction term (20) given by:

$$E^{si} = \sum_{i>j+2} sg(r_{ij}) \tag{9}$$

where

$$g(r_{ij}) = 1 - 0.5(7x^2 - 9x^3 + 5x^6 - x^8) \tag{10}$$

and $x = r_{ij}/9$, $r_{ij} < 9$ Å, and s = −0.8 kcal/mol.

E^{exv} is a side chain excluded volume term (21) that prevents the moving spheres from penetrating each other and is given by:

$$E^{\mathrm{exv}} = \sum_{i>j+2} V_{\mathrm{exv}}(r_{ij}), \tag{11}$$

$$V_{\mathrm{exv}}(r_{ij}) = \epsilon_{ij}\left[3\left(\frac{r_{ij}^0}{r_{ij}}\right)^8 - 4\left(\frac{r_{ij}^0}{r_{ij}}\right)^6 + 1\right], \tag{12}$$

for $r_{ij} < r_{ij}^0$ = 6.3 Å and ϵ_{ij} = 0.33 kcal/mol. This term is always positive as any attractive dispersive interactions are accounted for by other components of the total energy. The parameters for the last two terms are those given by Levitt (20) for threonine but were used here for all residues.

Penetration of the mobile residues into the volume of the fixed atoms in the protein was prevented by making corrections at each step. If, when moved, a sphere would fall within the excluded volume of the fixed atoms, then that sphere was returned to its original position and the pseudobonds in the moving loop were reconstrained. Overlaps between the spheres and the fixed atoms were then checked again and, if present, the correction procedure was repeated. This was continued until there were no unfavorable close contacts between the moving spheres and the fixed atoms or until the number of cycles of movements and reconstraints exceeded a predetermined number (5 during equilibration, 2 during data collection). In the latter case, the new positions of the spheres that satisfied the excluded volume criteria were used regardless of whether the bond constraints were satisfied.

Simulation methods

BD motion was simulated using the Ermak–McCammon equation (23) in which the position $\boldsymbol{r}_i$ of each residue i after a timestep of length Δt is given by:

$$\boldsymbol{r}_i = \boldsymbol{r}_i^0 + \frac{D_i \mathbf{F}_i^0}{kT}\Delta t + \mathbf{R}_i, \tag{13}$$

where k is Boltzmann's constant, T is absolute temperature, $\boldsymbol{r}_i^0$ is the initial position of residue i, D_i is its diffusion constant, $\mathbf{F}_i^0$ is the initial force on residue i, and $\mathbf{R}_i$ is its random displacement, which satisfies

$$\langle \mathbf{R}_i \rangle = 0, \tag{14}$$

$$\langle \mathbf{R}_i \mathbf{R}_i \rangle = 2D_i \Delta t \mathbf{I}. \tag{15}$$

The diffusion constant D_i is given by

$$D_i = \frac{kT}{6\pi\eta a_i}, \tag{16}$$

where η is the solvent viscosity (0.89 cp) and a_i is the hydrodynamic radius of residue i (3.15 Å).

A timestep, Δt, of 0.01 ps was used during equilibration with a harmonic bond potential. During data collection, SHAKE bond constraints were applied and a timestep of 0.03 ps was used. These timesteps were chosen after carefully monitoring the stability of the system for a number of short trajectories performed with different timesteps. They were the largest timesteps for which stability was retained and for

which there were not large fluctuations in the pseudobond lengths and angles or changes in the systematic forces on each residue during a single timestep. Each timestep took a similar amount of time with these two methods of evaluating bond contributions and so the use of bond constraints during data collection allowed a factor of three to be gained in simulation time.

Equilibration

Simulations were started with the spheres representing the residues of the loops centered on the positions of the CB atoms of the amino acid residues (or, in the case of glycine residues, the CA atoms) in the crystal structure. (Coordinates for the residues in the flexible loops had been assigned in the crystal structure [11] even though some of them were disordered.) Both the loops were in open conformations in the initial structure.

The system was first equilibrated to alleviate unfavourable contacts that arose because of the approximation of the shape of each loop residue as a sphere and because the geometry of the loops initially showed deviations from the equilibrium pseudobond lengths and angles. The system was equilibrated by performing a series of simulations of total time 720 ps at a temperature of 300 K. Each simulation was started using the final structure generated in the previous simulation and a different random number seed. When concatenated, these simulations were equivalent to one long simulation. A number of the spheres were initially within the excluded volume of the protein. To expel some of these, it was necessary, during the initial stages of equilibration, to displace them up to 2 Å further in the direction of the acting force than the distance given by the Ermak–McCammon equation. These extra displacements were required because the forces on the spheres (particularly the uncharged ones that moved independently of the fixed protein atoms) were insufficient to repel the spheres from the fixed protein atoms. In subsequent simulations, such additional movements were unnecessary.

Data collection

After equilibration, two simulations were performed: the first for 104 ns in the absence of salt and the second for 74 ns in a medium of 100 mM salt. The second simulation was started using the coordinates obtained after 72 ns of the first simulation. The simulations were performed as a series of runs with each run starting with the final coordinates of the previous one but with different random number seeds. Each run consisted of a maximum of 200,000 steps corresponding to 6 ns. Coordinates were recorded every 50 steps (1.5 ps). The total trajectory was then analyzed to examine the geometric properties of the loops and how they gate the active sites of the enzyme.

Simulations were carried out using the University of Houston Brownian Dynamics program (24, 25), which has been written as a general purpose program for electrostatic and BD calculations and which is available on request to the authors. Electrostatic calculations were performed on a Cray YMP and BD simulations were carried out on a Silicon Graphics 4D/320 workstation and a Cray YMP. A 6-ns simulation required ~7 h on a single processor of the Silicon Graphics computer.

Analysis

The "gating," i.e., the opening and closing of the active sites due to the motion of the loops, was assessed by monitoring the distance between CB Ser 211 and the five residues (169–173) at the center of each loop. These residues were chosen on the basis of crystallographic evidence concerning the interactions between the loops and ligands. Ser 211 is at the entrance of the active site on the opposite side from the flexible loop. In the crystal structures of the complexes of TIM with a number of ligands, it makes a hydrogen bond to the phosphate moiety of the ligand (9, 26). Thr 172 is the residue that is observed to undergo the largest displacement (≈7 Å) on ligand binding (9, 27). Gly 171 makes a hydrogen bond from its amide nitrogen to a phosphate oxygen of 2-phosphoglycolate on binding of this ligand to yeast TIM (9). Residues 169–173 also appear to retain the same conformation and act as a rigid body in the unliganded and liganded forms of the enzyme (9, 27).

When any of these five loop residues approached within 7 Å of CB Ser 211, the loop was assumed to have closed over the active site, preventing entrance of the substrate or exit of the product. When all of these residues moved away from CB Ser 211 a distance of ≥9 Å, the loop was assumed to have opened up sufficiently to allow the passage of ligands to and from the active site. However, to be described as open, the loop was required to remain open a minimum time of 100 ps before closing again. This was estimated as the time that was necessary for GAP to either enter or leave the active site, based on its diffusion constant relative to TIM of 0.1 $Å^2$/ps and the assumption that it must move 7–8 Å to leave the active site (the longest dimension of GAP is ~8 Å) using the following equation:

$$D = \lim_{t \to \infty} \frac{1}{6t} \langle (\Delta r)^2 \rangle. \quad (17)$$

The average times for which each loop was in open (τ_o) and closed (τ_c) conformations as well as the gating period (τ_{gate}) were calculated for each simulation.

RESULTS AND DISCUSSION

Gating characteristics

The simulations show that the peptide loops in both the subunits are able to act as gates closing over the active site. Their gating characteristics are given in Table 2.

Significant differences in the gating times and the conformations sampled in the presence and absence of salt were not detectable. There were, however, clear differences in the motions of the loops in the two subunits. In both 0 and 0.1 M salt solution, the loop in subunit I appears to move with a period of ~1 ns and to be closed over the active site for ~50% of the time, whereas the loop in subunit II appears to have a period of ~2 ns and to be closed for ~10% of the simulation time. Thus, the loop in subunit I was more mobile than that in subunit II and closed over the active site more often and for longer times.

Comparison of the motions of the peptide loops in subunits I and II

During the simulations, the loop in subunit I relaxed from its initial conformation so that all pseudobonds connecting the residues remained near their equilibrium length (5.14 Å) and bond angles fluctuated around 87° with a standard deviation of 5°. The whole loop was flexible, with dihedral angles taking values covering the full 360°, and with standard deviations in the range 121–148°, apart from the first dihedral, which varied over ~30°.

In subunit II, however, the pseudobonds between the terminal free residues and the adjacent fixed residues did not fully relax to their equilibrium lengths. They remained somewhat longer (5.4 and 5.8 Å) than the optimum length, although they were shorter than in the crystal structure (both 5.9 Å). Although the other bond an-

TABLE 2 **Gating characteristics of the simulated peptide loops of TIM**

Ionic strength	Subunit	No. of closures	Simulation time period*	Gating period τ_{gate}	Time closed τ_c‡	Time open τ_o‡	% Time open
M			*ns*	*ns*	*ps*	*ps*	
0.0	I	67	0–72	1.1	450.4 ± 615.4	620.8 ± 721.9	57.6
0.0	I	29	74–104	1.0	545.8 ± 685.5	480.7 ± 420.9	46.0
0.1	I	54	2–74	1.3	745.6 ± 1,177.5	553.2 ± 646.0	43.0
(0.1	I	19	2–26	1.3	583.2 ± 792.9	640.3 ± 409.3	52.3)
0.0	II	37	0–72	2.0	281.6 ± 415.5	1,578.7 ± 2,257.9	84.5
0.0	II	17	74–104	1.8	244.2 ± 359.7	1,528.4 ± 1,556.4	90.8
0.1	II	14	2–74	5.1	106.9 ± 156.8	4,457.2 ± 8,535.0	98.0
(0.1	II	12	2–26	2.0	115.7 ± 166.5	1,008.0 ± 1,446.8	89.7)
(0.1	II	1	26–50	24.0	4.5 ± 0.0	≈12,000.0 ± ≈5,000.00	100.0)

* The simulations in 0 mM salt were started from an equilibrated structure obtained after 720 ps simulation starting with the crystal structure. The simulations in 0.1 M salt were started with the loops in the conformation obtained after 72 ns simulation without any salt.
‡ Values are means ± standard deviations.

gles in the loop relaxed to 87° sd 5°, the first and last bond angles took values of ~71° and 98°, respectively. The strained geometry of the terminal free residues of the loop in subunit II was maintained because of excluded volume restrictions imposed by the surrounding protein. These restrictions prevented these residues from moving during the data collection simulations, although they did move during equilibration. These restrictions occurred even though the size of the excluded volume of the protein tends to be underestimated by an amount that is dependent on the grid spacing. The excluded volume was calculated with a probe of radius 2 Å (representative of a methyl group), which is smaller than the hydrodynamic radius (3.15 Å) of each residue and was chosen to allow for neglected flexibility in the protein core and in the sidechains of the residues of the loop.

The other free residues in the loop in subunit II moved quite freely (e.g., for residue 167, dihedral ϕ_4 moved through 120° and for residue 175, dihedral ϕ_{15} moved through 75°). The standard deviation in the dihedrals ranged from 26 to 158° for all except the first and last dihedral angles, which were constant. Nevertheless, the loop in subunit II sampled fewer conformations than that in subunit I. This is because in subunit II, there were effectively only 9 moving residues, whereas in subunit I all 11 residues of the loop moved throughout the simulations. Crystallographic data (27) suggest that the flexible loop is longer than nine residues and, therefore, the simulation of the loop in subunit I would appear to be more consistent with the experimental data.

Both the loops moved as flexible chains rather than rigid bodies. The rigid flap movements referred to in crystallographic (9, 27) and other theoretical (14) studies were not detected in these simulations. In all simulations, when the loops were in open conformations, they tended to extend out into solution more than they do in the crystal structure. Subunit I adopted a more open structure (Fig. 3); for example, the average distance between residues 166 and 176 was 13.5 Å in subunit I but only 6.3 Å in subunit II. Average distances between residues 169 and 174 were also longer in subunit I than in subunit II and were longer than observed in the chicken and yeast TIM crystal structures (~5 Å). In the yeast crystal structure (8), the distance between these residues is approximately constant when the loop is in open and closed conformations and the intervening residues appear to form a rigid flap.

The differences in the motion of the two loops seen in the simulations appear to stem from differences between the two subunits in the crystal structure. When superimposed, subunits I and II of the chicken TIM dimer differ most in the region of the flexible loops and at the two amino- and five carboxyl-terminal residues. The β-sheet extending up to residue 167 shows little difference in the two subunits, but from residue 168 onward, differences

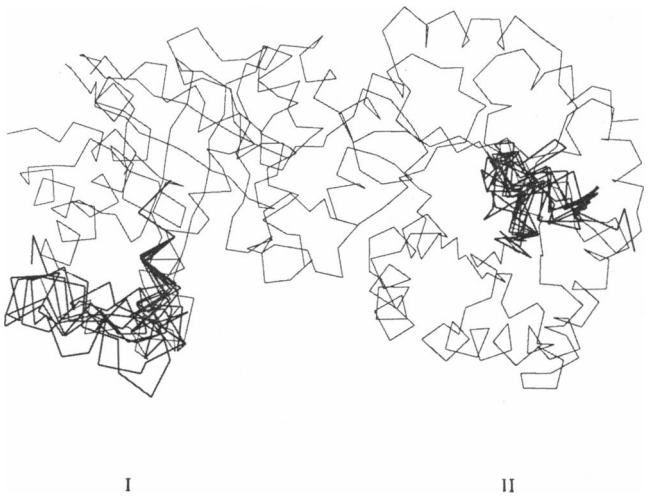

FIGURE 3 Ten snapshots at intervals of 6 ns for part of the simulation in the absence of salt solution. The loop in subunit I samples a greater volume of conformational space than the loop in subunit II.

start to be noticable. The CA atoms of Thr 172 differ by 2.5 Å and of Gly 171 by 3.5 Å with the loop in subunit I being more closed than in subunit II. The α-helix extending beyond residue 176 is ~0.7 Å more buried in subunit II than subunit I. Ser 211, which is here used to define gating properties, is 0.7 Å further from the loop and closer to the rest of the protein in subunit II than subunit I. All of these differences may make the closing of the loop in subunit II less probable than in subunit I.

In the electron density map (7, 11, 12) of chicken TIM, residues 168–176 are disordered in subunit I and exposed to solvent, but in subunit II they are observed in a defined open conformation that is maintained by contacts with other molecules in the crystal. Sulphate and phosphate ions can bind in the active site of subunit I but not subunit II in the crystal structure (12). These differences suggest that the loop in subunit I may undergo motions that are more like those of the enzyme in solution in its active form than the loop in subunit II, which exists in a somewhat artificial state that hinders its motion.

The gating characteristics of the loop in subunit I are also more uniform throughout the simulations. Therefore, as the loop in subunit I appeared to be more representative of the loop motion of the active enzyme in solution, the rate constants given in the following section were only calculated for the loop in subunit I.

Gated rate constant

Each peptide loop may be considered as a gate that can exist in one of two states: open or closed (28–30). Rate constants k_o and k_c describe the transitions between the two states according to the following kinetic scheme:

$$\text{open} \underset{k_o}{\overset{k_c}{\rightleftharpoons}} \text{closed}. \qquad (18)$$

The stochastically gated rate constant, k, for the association of the substrate and the protein in the presence of these loops can be derived by solving diffusion equations for the substrate, subject to suitable boundary conditions (30). It is given by the following equation:

$$k^{-1} = k_\infty^{-1} + [k_c^{-1} k_o (k_o + k_c) \hat{\kappa}_u (k_o + k_c)]^{-1}, \qquad (19)$$

where $\hat{\kappa}_u(s)$ is the Laplace transform of the time-dependent rate constant for the ungated protein and k_∞ is the steady-state rate constant for the ungated protein. For a diffusion controlled reaction, $k_\infty = k_D$.

The diffusional relaxation time of the enzyme-substrate system, τ_d, is given by

$$\tau_d \equiv R^2/D \approx (40^2)/0.1 = 16{,}000 \text{ ps} = 16 \text{ ns}, \qquad (20)$$

where R is the distance between the molecular centers of TIM and GAP at contact and D is their relative diffusion constant. The gating period ($\approx$1 ns) is much shorter than the diffusional relaxation time. For this case of a rapidly gated, diffusion-controlled reaction, the gated rate constant k is simply given by the rate constant k_D for the enzyme with the gate held open as the second term on the right-hand side of Eq. 19 becomes negligible (30):

$$k = k_D, \quad (k_o + k_c)^{-1} \ll \tau_d \qquad (21)$$

Thus, when gating is sufficiently fast and the association is diffusion controlled, it appears to the substrate that the gates on the protein are always open.

The strength of the salt solution appears to have little effect on the loop motions, although a longer simulation at a much higher salt concentration might reveal different peptide loop motions. This is probably because only one of the moving residues in each loop has a formal charge (Lys 174) and other forces on the loop residues are therefore of greater importance. Simulations with a more realistic model, in which each residue was modeled by more than one center with a partial charge might be more dependent on salt concentration. These simulations also suggest that the viscosity dependence of the rate constant for TIM is likely to arise from dynamical effects on the approach of substrate rather than dynamical effects on the peptide loops.

The model of the flexible loops used here was extensively tested during development (20, 21). Nevertheless, the further optimization of parameters and force-field terms may lead to an improved model. Moderate adjustments of parameters are, however, unlikely to alter the finding that the gating period of the loops is much smaller than the substrate-enzyme relaxation time and, therefore, that the reaction rate constant is unaffected by gating.

CONCLUSIONS

Simulations of the peptide loops near the active sites of the enzyme TIM show that they can act as gates but that they do not lead to a reduction in the rate constant for the diffusion-controlled, substrate-enzyme association. Thus, their motion does not account for the difference between the experimental rate constant and the rate constant calculated earlier by BD (4), neglecting the motion of the loops. This suggests that there are also other components of the enzyme-substrate system that are important in determining the rate constant that were not included in the model used for the previous calculations. For example, the substrate was modeled as a sphere with a point charge, but its asymmetric shape and charge may play important roles in steering the substrate into the active site. In addition, the criteria for defining an enzyme-substrate reaction may not have been sufficiently stringent. Indeed, we recently have found that the rate constant drops to the right order of magnitude when the orientational requirements for substrate binding are considered (31). Thus, it appears that the flexible loops, which are needed to create the catalytic environment in

TIM, have evolved to minimize the potentially adverse effects associated with gating of the active sites.

This work was supported by grants from the National Science Institutes of Health, the Robert A. Welch Foundation, the National Center for Supercomputing Applications, and the San Diego Supercomputer Center. J. A. McCammon is the recipient of the George H. Hitchings Award from the Burroughs Wellcome Fund.

Received for publication 20 May 1992 and in final form 8 September 1992.

REFERENCES

1. Albery, W. J., and J. R. Knowles. 1976. Free-energy profile for the reaction catalysed by triose phosphate isomerase. *Biochemistry.* 25:5627–5631.
2. Blacklow, S. C., R. T. Raines, W. A. Lim, P. D. Zamore, and J. R. Knowles. 1988. Triosephosphate isomerase catalysis is diffusion controlled. *Biochemistry.* 27:1158–1167.
3. Knowles, J. R. 1991. Enzyme catalysis: not different, just better. *Nature (Lond.).* 350:121–124.
4. Madura, J. D., and J. A. McCammon. 1989. Brownian dynamics simulation of diffusional encounters between triose phosphate isomerase and d-glyceraldehyde phosphate. *J. Phys. Chem.* 93:7285–7287.
5. Alber, T., W. A. Gilbert, D. Ringe Ponzi, and G. A. Petsko. The role of mobility in the substrate binding and catalytic machinery of enzymes. *In* Mobility and Function in Proteins and Nucleic Acids. Pitman, London. 1983. 4–24.
6. Pompliano, D. L., A. Peyman, and J. R. Knowles. 1990. Stabilization of a reaction intermediate as a catalytic device: definition of the functional role of the flexible loop in triosephosphate isomerase. *Biochemistry.* 29:3186–3194.
7. Banner, D. W., A. C. Bloomer, G. A. Petsko, D. C. Phillips, C. I. Pogson, I. A. Wilson, P. H. Corran, A. J. Furth, J. D. Milman, R. E. Offord, J. D. Priddle, and S. G. Waley. 1975. Structure of chicken muscle triose phosphate isomerase determined crystallographically at 2.5 Å resolution using amino acid sequence data. *Nature (Lond.).* 255:609–614.
8. Lolis, E., T. Alber, R. C. Davenport, D. Rose, F. C. Hartman, and G. A. Petsko. 1990. Structure of yeast triosephosphate isomerase at 1.9å resolution. *Biochemistry.* 29:6609–6618.
9. Lolis, E., and G. A. Petsko. 1990. Crystallographic analysis of the complex between triosephosphate isomerase and 2-phosphoglycolate at 2.5 Å resolution: implications for catalysis. *Biochemistry.* 29:6619–6625.
10. Wierenga, R. K., M. E. M. Noble, G. Vriend, S. Nauche, and W. G. J. Hol. 1991. Refined 1.83 Å structure of the trypanosomal triosophosphate isomerase crystallized in the presence of 2.4 m-ammonium sulphate. *J. Mol. Biol.* 220:995–1015.
11. Banner, D. W., A. C. Bloomer, G. A. Petsko, D. C. Phillips, and I. A. Wilson. 1976. Atomic coordinates for triose phosphate isomerase from chicken muscle. *Biochem. Biophys. Res. Commun.* 72:146–155.
12. Alber, T., D. W. Banner, A. C. Bloomer, G. A. Petsko, D. C. Phillips, P. S. Rivers, and I. A. Wilson. 1981. On the three-dimensional structure and catalytic mechanism of triose phosphate isomerase. *Philos. Trans. R. Soc. Lond. B. Biol. Sci.* 293:159–171.
13. Bernstein, F. C., T. F. Koetzle, G. J. B. Williams, E. F. Meyer, M. D. Brice, J. R. Rodgers, O. Kennard, T. Shimanouchi, and M. Tasumi. 1977. The protein data base: a computer-based archival file for macromolecular structures. *J. Mol. Biol.* 112:535–542.
14. Joseph, D., G. A. Petsko, and M. Karplus. 1990. Anatomy of a conformational change: hinged 'lid' motion of the triosephosphate isomerase loop. *Science (Wash. DC).* 249:1425–1428.
15. *QUANTA* Molecular Modeling Software Package. 1992. Molecular Simulations, Inc., Waltham, MA.
16. Jorgensen, W. L., and J. Triado-Rives. 1988. The opls potential functions for proteins. energy minimizations for crystals of cyclic peptides and crambin. *J. Am. Chem. Soc.* 110:1657–1666.
17. Davis, M. E., and J. A. McCammon. 1989. Solving the finite difference linearized Poisson-Boltzmann equation: a comparison of relaxation and conjugate gradient methods. *J. Comput. Chem.* 10:386–391.
18. Davis, M. E., and J. A. McCammon. 1991. Dielectric boundary smoothing in finite difference solutions of the Poisson equation: an approach to improve accuracy and convergence. *J. Comput. Chem.* 7:909–912.
19. Levitt, M., and A. Warshel. 1975. Computer simulation of protein folding. *Nature (Lond.).* 253:694–698.
20. Levitt, M. 1976. A simplified representation of protein conformations for rapid simulation of protein folding. *J. Mol. Biol.* 104:59–107.
21. McCammon, J. A., S. H. Northrup, M. Karplus, and R. M. Levy. 1980. Helix-coil transitions in a simple polypeptide model. *Biopolymers.* 19:2033–2045.
22. Ryckaert, J. P., G. Ciccotti, and H. J. C. Berendsen. 1977. Numerical integration of the cartesian equations of motion of a system with constraints: molecular dynamics of n-alkanes. *J. Comput. Phys.* 23:327–341.
23. Ermak, D. L., and J. A. McCammon. 1978. Brownian dynamics with hydrodynamic interactions. *J. Chem. Phys.* 69:1352–1360.
24. Davis, M. E., J. D. Madura, B. A. Luty, and J. A. McCammon. 1990. Electrostatics and diffusion of molecules in solution: simulations with the University of Houston Brownian dynamics program. *Comp. Phys. Comm.* 62:187–197.
25. Davis, M. E., J. D. Madura, J. Sines, B. A. Luty, S. A. Allison, and J. A. McCammon. 1991. Diffusion-controlled enzymatic reactions. *Methods Enzymol.* 202:473–497.
26. Noble, M. E. M., R. K. Wierenga, A-M. Lambert, F. R. Opperdoes, A-M. W. H. Thunnissen, K. H. Kalk, H. Groendijk, and W. G. J. Hol. 1991. The adaptability of the active site of trypanosomal triosephosphate isomerase as observed in the crystal structures of three different complexes. *Proteins.* 10:50–69.
27. Wierenga, R. K., M. E. M. Noble, J. P. M. Postma, H. Groendijk, K. H. Kalk, W. G. J. Hol, and F. R. Opperdoes. 1991. The crystal structure of the open and the closed conformation of the flexible loop of trypanosomal triosephosphate isomerase. *Proteins.* 10:33–49.
28. McCammon, J. A., and S. H. Northrup. 1981. Gated binding of ligands to proteins. *Nature (Lond.).* 293:316–317.
29. Northrup, S. H., F. Zarin, and J. A. McCammon. 1982. Rate theory for gated diffusion-influenced ligand binding to proteins. *J. Phys. Chem.* 86:2314–2321.
30. Szabo, A., D. Shoup, S. H. Northrup, and J. A. McCammon. 1982. Stochastically gated diffusion-influenced reactions. *J. Chem. Phys.* 77:4484–4493.
31. Luty, B. A., R. C. Wade, J. D. Madura, M. E. Davis, J. M. Briggs., and J. A. McCammon. 1993. Brownian dynamics simulations of diffusional encounters between triose phosphate isomerase and glyceraldehyde phosphate: electrostatic steering of glyceraldehyde phosphate. *J. Phys. Chem.* In press.